Factors affecting the Assembly of Helical and Non-helical Zinc(II) Bipyridyl Metallomacrocycles†

Alexander Bilyk, Margaret M. Harding,* Peter Turner and Trevor W. Hambley
School of Chemistry, University of Sydney, N.S.W. 2006, Australia

The assembly of a non-helical bimetallic [2 + 2] macrocyclic complex between two zinc(II) atoms and two bis(bipyridyl) compounds containing a 2,7-disubstituted pyrene linker, previously assigned by dynamic NMR spectroscopy, has been confirmed by X-ray crystallography. The crystal structure of bis{2,7-bis[3-(6'-methyl-2,2'-bipyridin-6-yl)-2-oxapropyl]pyrene}dizinc tetrakis(trifluoromethanesulfonate) was determined by X-ray diffraction methods and refined to a residual of 0.092 for 1916 independent observed reflections: triclinic, space group $P\bar{1}$, $a = 16.333(6)$, $b = 18.934(5)$, $c = 10.004(1)$ Å, $\alpha = 100.96(2)$, $\beta = 97.33(2)$, $\gamma = 110.71(2)°$. The two zinc(II) ions are bound to four nitrogens from two bipyridyl groups and two oxygen atoms from the ether links in a distorted-octahedral geometry. A non-helical geometry is observed and the two pyrene rings are offset by 3.84 Å and separated by 3.65 Å. A related compound, in which a 1,4-disubstituted benzene linker is used in place of pyrene, has also been prepared, and in solution this forms approximately equal amounts of helical and non-helical complexes with zinc(II). The relative stabilities of helical and non-helical complexes formed between 6,6'-disubstituted bis(bipyridyl) ligands connected by 2,7-disubstituted pyrene, 2,6-disubstituted naphthalene and 1,4-disubstituted benzene are discussed.

The importance of metal ions in the controlled assembly of supramolecular structures is now well recognized.[1,2] Key features which determine the outcome of the assembly process are the ligand design, flexibility of the linker groups joining the co-ordination sites, and the stereochemical preferences of the co-ordinating metal ion.[1-8] Double and triple helical complexes and other structures have been reported using Ni^{II}, Cu^{I}, Ag^{I}, Mn^{II} and Pd^{II}.[2-8] In contrast, there are few examples of zinc(II) in this context. Williams and co-workers[6-8] have assembled double and triple helices from benzimidazole ligands with a range of metal ions. In studies carried out with zinc(II), mixtures of complexes were obtained, which was attributed to the lack of stereochemical preference of the spherical d^{10} zinc(II) ion.[7] There is one example of helical complex formed from zinc(II) and a biliverdin dimethyl ester.[9]

Our interest in this area has been in the application of co-ordination chemistry to the assembly of macrocyclic complexes of defined shape and structure from two ligand molecules and two metal ions. To this end we reported the assembly of [2 + 2] bimetallic macrocycles from bis(bipyridyl) compounds L^1 and L^2 and the metal ions Cu^{I} and Zn^{II}.[10] The relative amounts of helical and non-helical complexes was found to be dependent on both the co-ordinating metal ion and the structure of the aromatic linker. In the presence of Zn^{II}, L^1 was observed to form exclusively one complex, which was assigned as the non-helical complex **1**, on the basis of variable-temperature NMR data.[10] We now report the crystal structure of **1** which confirms our NMR assignment and reveals unusual structural features of zinc(II) bis(bipyridyl) complexes which favour the formation of the non-helical complex **1**. The co-ordination chemistry of the three related bis(bipyridyl) compounds L^1–L^3 is compared, in order to determine what factors control the assembly of both helical and non-helical [2 + 2] bimetallic macrocyclic complexes.

Results and Discussion

Crystal Structure.—Crystals of $[Zn_2L^1{}_2][CF_3SO_3]_4$ **1**, after many attempts, were obtained by slow diffusion of diethyl ether into an acetonitrile solution of the complex. An ORTEP[11] depiction of the crystal structure and space-filling representation are shown in Figs. 1 and 2. The solid-state complex has a non-helical configuration, in agreement with the solution structure,[10] which we had tentatively assigned on the basis of dynamic NMR spectroscopic studies. The relative lateral offset of the pyrene rings is 3.84 Å and they are separated by 3.65 Å. The Zn • • • Zn distance is 14.42 Å (Fig. 1) and each zinc(II) ion is six-co-ordinated to two bipyridyl groups and two oxygen atoms of the ether linkers. The co-ordination is best described as distorted octahedral, having a *cis* distortion and both out-of-plane and off-axis binding. The zinc co-ordination bond lengths are given in Fig. 3 which depicts the distorted co-ordination sphere. Positional parameters and bond angles are listed in Tables 1 and 2 The configurations at the metal centres are opposite (Δ,Λ),[12] resulting in an achiral, non-helical complex.‡

Not surprisingly, given the geometry of the tridentate ligand system, the bonds between the comparatively soft Lewis-acid metal and the soft bipyridine base are shorter than the bonds to the harder ether oxygen atoms. In chelating the zinc(II) ions, the bipyridine least-squares plane of ligand A forms a dihedral angle of 84° with the equivalent plane of ligand B. The methyl groups have a 3.43(4) Å contact with a carbon site on the opposing bipyridyl residue, and do not impede the zinc chelation. The bipyridyl residues deviate slightly from planarity, with the 13(4)° torsion angle between the pyridyl components of ligand A being larger than the 4(5)° angle of B. The range of deviations from the bipyridyl least-squares planes is 0.02–0.15 Å for ligand A, and 0.00–0.03 Å for B. The zinc is slightly displaced from the bipyridyl least-squares planes of ligands A and B by 0.03 and 0.09 Å respectively. The ether oxygen atoms are also

† *Supplementary data available:* see Instructions for Authors, *J. Chem. Soc., Dalton Trans.*, 1994, Issue 1, pp. xxiii–xxviii.

‡ Owing to the octahedral geometry about the zinc ions, the *R* and *S* assignments made previously (see ref. 10) for tetrahedral complexes are inappropriate and the Δ and Λ notations have been used. The configurational assignments at each zinc centre were assigned as for any bis(bidentate ligand) octahedral complex.[12] Both non-helical, achiral complexes (Δ and Λ) or (Λ and Δ) and chiral, helical complexes (Λ and Λ) or (Δ and Δ) are possible.

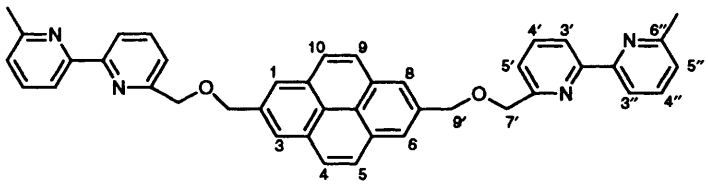

L^1

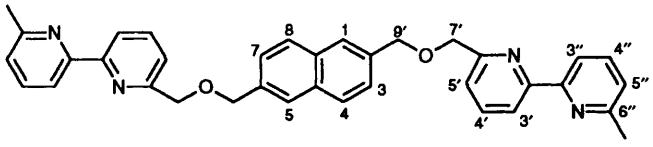

L^2

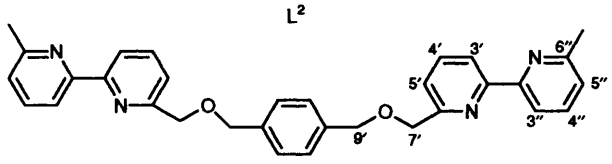

L^3

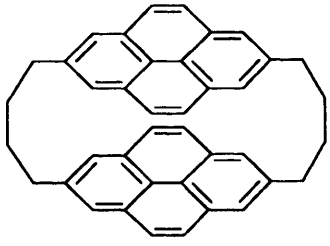

I

essentially located in the bipyridyl least-squares planes, with the deviation being 0.03 Å for ligand A and 0.10 Å for B.

6.6′-Dimethyl-2,2′-bipyridine and other 6,6′-disubstituted-2,2′-bipyridines destabilize square-planar co-ordination and tetrahedral and octahedral co-ordination are typically observed with a range of metals.[13] To our knowledge, there are no examples of crystal data for zinc(II) complexes of 6,6-disubstituted bipyridyl ligands. The crystal structure of complex **1** shows some similarity to that of the *cis* distorted-octahedral bis(2,2′-bipyridyl)nitritozinc(II) nitrate.[14] However, the octahedral distortion in **1** is considerably more pronounced than that observed in this structure.

Solution Structure of Complex **1**.—In view of the crystal structure of complex **1**, NMR spectroscopy was used to establish whether the same structural features were present in solution as in the solid state. The ^{1}H NMR spectrum was fully assigned using correlation spectroscopy (COSY)[15] and nuclear Overhauser enhancement spectroscopy (NOESY)[16] experiments. As previously reported,[10] at room temperature, the pyrene rings are rotating slowly on the NMR time-scale. At low temperature the observed chemical shift differences are consistent with the offset non-helical structure found in the solid state (Fig. 1). The NOESY spectra were recorded at low temperature (235 K) where all aromatic resonances appeared as sharp signals. The expected proton connectivities were detected, but in addition several long range nuclear Overhauser enhancements (NOEs) were observed (Fig. 4, Table 3). These NOEs are consistent with the structure observed in the solid state and confirm the co-ordination of the oxygen atoms to the zinc centres. Of particular importance, two weak NOEs were observed from $H^{5'}$ on the bipyridyl ring of ligand A to the pyrene protons $H^{4,5}$ and $H^{3,6}$ on ligand B (Fig. 2). The methylene protons ($H^{7'a,b}$) also gave a strong NOE to the pyrene protons. These NOEs arise due to the octahedral geometry that places the methylene protons and one half of the bipyridyl ring very close to the pyrene-ring protons (Fig. 2). In the corresponding tetrahedral complex formed with copper(I), model building shows that $H^{7'a,b}$ are placed away from the pyrene ring, and in the corresponding NOESY experiment long-range NOEs between $H^{7'a,b}$ and the pyrene-ring protons were not observed.

Further evidence for the octahedral co-ordination in complex **1** is given by the large chemical shift differences of the methylene protons $H^{7'a,b}$ and $H^{9'a,b}$ (Fig. 4). The diastereotopic methylene protons $H^{7'a,b}$ resonate at $\delta \approx 5$, *i.e.* at a similar chemical shift to the corresponding protons in the uncomplexed L^1. In contrast, protons $H^{9'a,b}$ are shifted upfield by ≈ 1 ppm (CD_3CN: δ 3.92 and 4.43). From the crystal structure (Fig. 2), co-ordination of the ether oxygens to the zinc(II) atoms results in protons $H^{9'a,b}$ being shielded by the bipyridyl group on the second ligand molecule (Fig. 2). The chemical shift of these protons is quite different to those observed in the corresponding copper(I) complex, where the tetrahedral co-ordination at each of the copper(I) centres results in both $H^{7'}$ and $H^{9'}$ being shielded by a similar amount and both sets of protons resonate at $\delta \approx 3$–4.[10]

NMR Assignment of Helical and Non-helical Octahedral Complexes.—The preparation of the zinc(II) complexes of compounds L^1 and L^2, **1** and **2**, respectively, have previously been reported, but the co-ordination at each zinc(II) centre was incorrectly assumed to be tetrahedral.[10] Variable-temperature NMR data for **1** and the crystal structure reported in this work show conclusively that L^1 forms exclusively the non-helical complex **1** with zinc(II). In contrast, a mixture of two complexes, **2a** and **2b**, was detected when L^2 was treated with zinc(II).[10] Ligand L^3, which contains a 1,4-disubstituted benzene linker, and the corresponding zinc(II) complex **3**, were prepared in this work, in order to assess the role of the aromatic spacer on the types of complexes formed with zinc(II).

Both complexes **2** and **3**, which contain naphthalene and

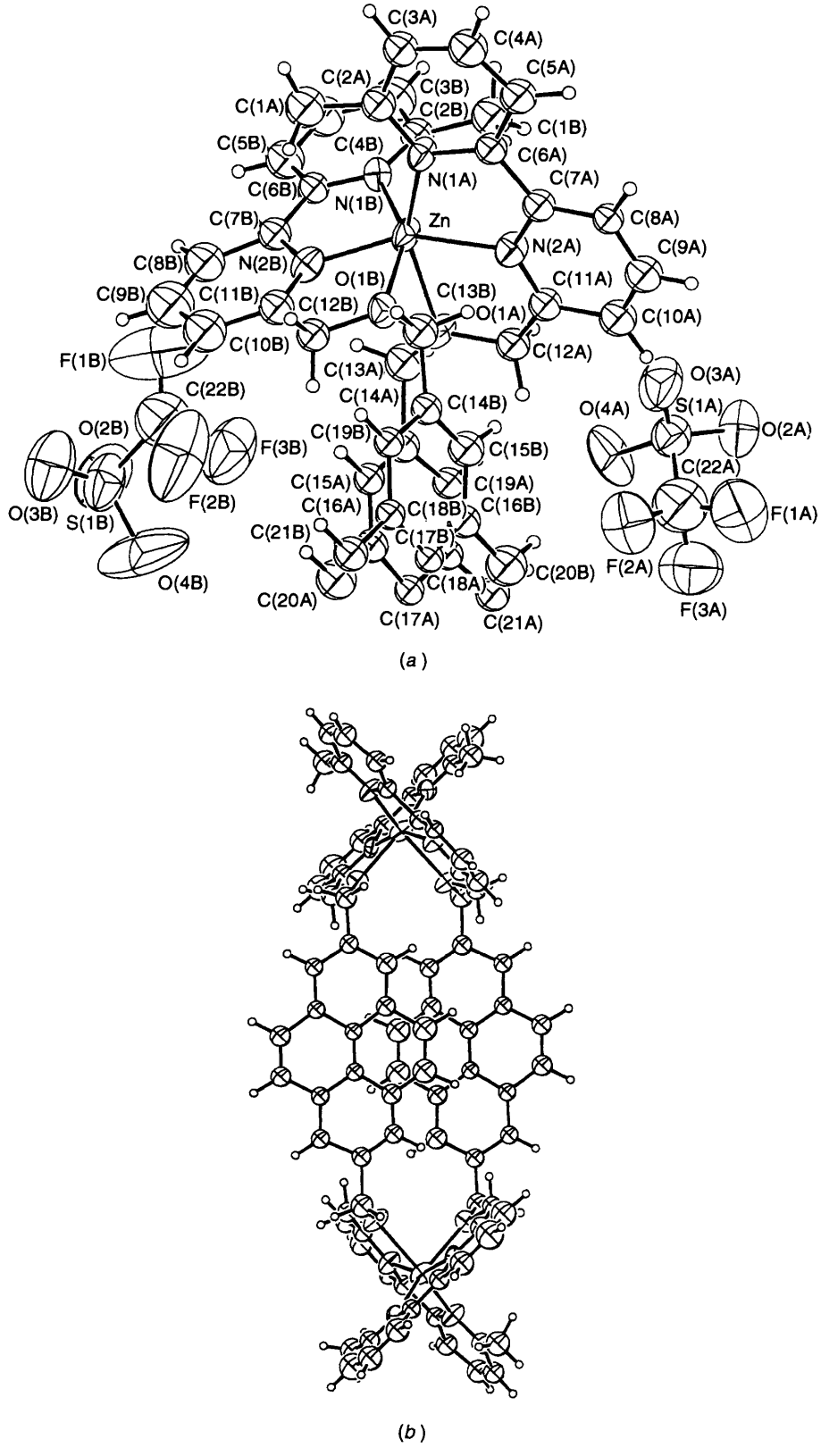

(*a*)

(*b*)

Fig. 1 An ORTEP depiction and numbering scheme of (*a*) the asymmetric unit of $[Zn_2L^1{}_2]^{4+}$, (*b*) the full cation $[Zn_2L^1{}_2]^{4+}$; thermal ellipsoids are drawn at the 25% level

benzene spacers respectively, were assumed to have similar structures to that of **1**, in which zinc(II) is octahedrally co-ordinated as shown in Fig. 3. Strong evidence for this type of co-ordination in solution is the chemical shifts of the methylene protons in **2** and **3**. For each complex, $H^{9'a,b}$ resonate at $\delta \approx 5$ while $H^{7'a,b}$ are shifted upfield to $\delta \approx 4$. As discussed above, this behaviour is entirely consistent with octahedral co-ordination, and would not be expected if tetrahedral (or other) co-ordination types were present.

Variable-temperature NMR experiments were carried out on

Table 1 Positional parameters for $[Zn_2L^1{}_2][CF_3SO_3]_4$ **1**

Atom	*x*	*y*	*z*	Atom	*x*	*y*	*z*
Zn	0.2791(3)	0.7367(2)	0.2635(3)	C(22A)	0.083(5)	0.342(4)	0.475(8)
S(1A)	0.0292(8)	0.3955(6)	0.495(1)	C(23)[a]	0.199(6)	0.254(5)	0.06(1)
F(1A)	0.052(2)	0.279(2)	0.357(3)	N(1B)	0.227(2)	0.811(1)	0.386(2)
F(2A)	0.173(2)	0.373(1)	0.453(2)	F(1B)	0.494(3)	0.926(2)	0.908(4)
F(3A)	0.096(2)	0.298(2)	0.559(3)	S(1B)	0.617(1)	0.9028(8)	1.082(1)
O(1A)	0.268(1)	0.6561(8)	0.414(1)	C(1B)	0.071(2)	0.738(2)	0.248(3)
O(2A)	−0.061(2)	0.342(1)	0.490(2)	O(1B)	0.394(1)	0.7040(8)	0.208(1)
O(3A)	0.037(2)	0.429(1)	0.380(3)	N(2B)	0.392(2)	0.814(1)	0.399(2)
O(4A)	0.082(1)	0.445(1)	0.627(2)	F(2B)	0.579(3)	0.837(2)	0.838(3)
O(5)[a]	0.143(4)	0.292(3)	0.025(6)	C(2B)	0.147(2)	0.799(2)	0.363(3)
O(6)[a]	0.258(4)	0.203(4)	0.541(7)	O(2B)	0.580(2)	0.916(2)	1.186(3)
N(1A)	0.254(1)	0.760(1)	0.067(2)	F(3B)	0.475(2)	0.804(1)	0.940(2)
N(2A)	0.190(1)	0.627(1)	0.154(2)	C(3B)	0.116(2)	0.850(2)	0.457(4)
C(1A)	0.345(2)	0.899(2)	0.141(3)	O(3B)	0.680(2)	0.960(2)	1.066(3)
C(2A)	0.281(2)	0.829(2)	0.032(3)	C(4B)	0.190(2)	0.909(2)	0.563(3)
C(3A)	0.247(2)	0.835(1)	−0.097(3)	O(4B)	0.630(3)	0.822(2)	1.072(5)
C(4A)	0.189(2)	0.769(2)	−0.194(3)	C(5B)	0.273(2)	0.916(2)	0.580(3)
C(5A)	0.155(2)	0.697(1)	−0.162(3)	C(6B)	0.291(2)	0.865(1)	0.483(3)
C(6A)	0.191(2)	0.696(1)	−0.031(3)	C(7B)	0.376(2)	0.871(1)	0.500(3)
C(7A)	0.163(2)	0.621(1)	0.014(3)	C(8B)	0.461(2)	0.921(2)	0.595(3)
C(8A)	0.115(1)	0.547(1)	−0.076(2)	C(9B)	0.541(3)	0.923(2)	0.597(4)
C(9A)	0.098(2)	0.484(1)	−0.021(3)	C(10B)	0.555(2)	0.868(2)	0.487(3)
C(10A)	0.123(2)	0.489(1)	0.117(3)	C(11B)	0.471(2)	0.814(2)	0.393(3)
C(11A)	0.175(2)	0.567(2)	0.209(3)	C(12B)	0.482(2)	0.755(1)	0.286(3)
C(12A)	0.200(2)	0.580(1)	0.362(3)	C(13B)	0.399(2)	0.648(1)	0.092(3)
C(13A)	0.292(2)	0.679(1)	0.564(3)	C(14B)	0.442(2)	0.596(1)	0.136(2)
C(14A)	0.345(2)	0.629(1)	0.618(2)	C(15B)	0.400(2)	0.541(1)	0.207(3)
C(15A)	0.426(2)	0.637(1)	0.600(2)	C(16B)	0.449(2)	0.499(1)	0.255(2)
C(16A)	0.465(2)	0.595(1)	0.643(2)	C(17B)	0.531(2)	0.505(1)	0.239(2)
C(17A)	0.427(2)	0.538(1)	0.718(2)	C(18B)	0.570(2)	0.562(1)	0.168(2)
C(18A)	0.341(2)	0.528(1)	0.732(2)	C(19B)	0.527(2)	0.606(1)	0.118(2)
C(19A)	0.295(2)	0.571(1)	0.686(2)	C(20B)	0.407(2)	0.440(2)	0.329(3)
C(20A)	0.546(2)	0.603(2)	0.627(3)	C(21B)	0.660(2)	0.571(1)	0.155(2)
C(21A)	0.295(2)	0.469(1)	0.796(2)	C(22B)[b]	0.5350	0.8816	0.9402

[a] Occupancy 0.5; all the other atomic sites are fully occupied. [b] Fixed atom.

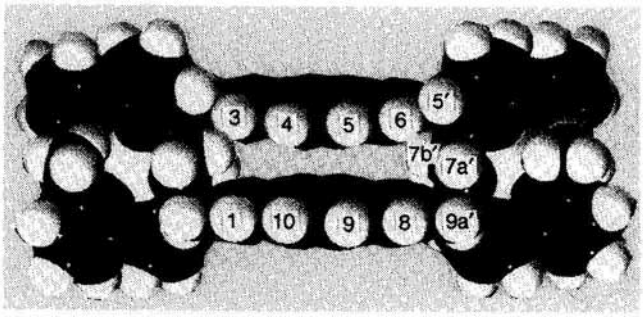

Fig. 2 Space-filling representation of the cation $[Zn_2L^1{}_2]^{4+}$ showing the cavity

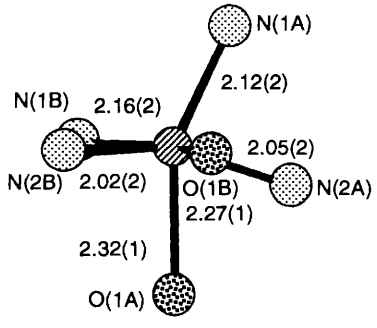

Fig. 3 Bond lengths (Å) and geometry at each zinc(II) centre in complex **1**

Table 2 Zinc bond angles (°) for $[Zn_2L^1{}_2][CF_3SO_3]_4$ **1**

O(1A)–Zn–N(1A)	153.9(6)	N(1A)–Zn–N(2B)	116.0(7)
O(1A)–Zn–N(2A)	73.0(6)	N(2A)–Zn–N(1B)	117.3(8)
O(1A)–Zn–N(1B)	94.1(6)	N(2A)–Zn–O(1B)	89.5(6)
O(1A)–Zn–O(1B)	85.9(5)	N(2A)–Zn–N(2B)	155.0(8)
O(1A)–Zn–N(2B)	87.7(6)	N(1B)–Zn–O(1B)	152.1(7)
N(1A)–Zn–N(2A)	81.1(7)	N(1B)–Zn–N(2B)	79.1(9)
N(1A)–Zn–N(1B)	100.8(7)	O(1B)–Zn–N(2B)	73.0(7)
N(1A)–Zn–O(1B)	90.6(6)		

Estimated standard deviations in the least significant figure are given in parentheses.

complexes **2** and **3** and in each case, two sets of aromatic signals were detected (Figs. 5 and 6). For **2**, as the temperature is lowered, the more downfield set of the naphthalene protons, assigned as **2a**, broadened (*e.g.*, $H^{3,7}$ in Fig. 5), while the signals due to **2b** remained sharp in the temperature range 190–300 K. A similar pattern was observed for complex **3** (Fig. 6) and two singlets for the benzene protons in the helical and non-helical complexes, **3a** and **3b**, were observed. As the temperature was lowered the more downfield signal, assigned to **3a**, broadened while the signal due to **3b** remained sharp (Fig. 6). All of the bipyridyl proton resonances of **2** and **3** remained sharp in the range 180–300 K. The dynamic behaviour of only one set of aromatic resonances suggests that there is restricted rotation of the aryl rings in both **2a** and **3a** compared to **2b** and **3b** respectively.

In the non-helical complex **1** the pyrene rings are in close proximity to one another, separated by 3.65 Å (Fig. 2). However, these rings retain torsional flexibility and are observed to rotate slowly on the NMR time-scale.[10] The corresponding helical complex **1a** was constructed with the aid of molecular modelling, assuming a similar distorted-octahedral

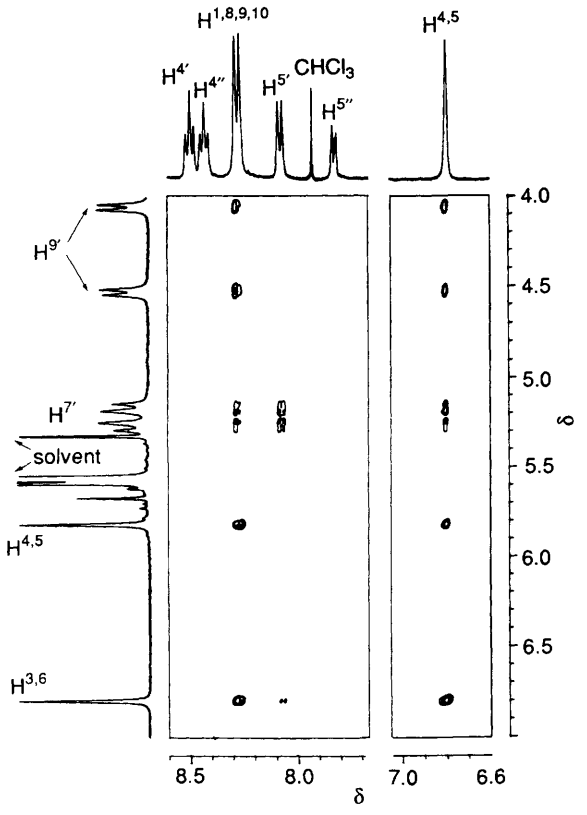

Fig. 4 Section of the 400 MHz NOESY spectrum of complex **1** in CD_3OD at 235 K with a mixing time of 200 ms; for assignments refer to Fig. 2

Table 3 Connectivities observed in a NOESY experiment (τ_m = 200 ms) on complex **1** in CD_3OD at 230 K; w = weak signal

Irradiated proton	Observed NOEs
H^1, H^8, H^9, H^{10}	H^3, H^4, H^5, H^6, $H^{7'}$, $H^{9'}$
H^3,H^6	H^1, H^4, H^5, H^8, H^9, H^{10}, $H^{7'}$, $H^{9'}$, $H^{5'}$(w)
H^4, H^5	H^1, H^3, H^6, H^8, H^9, H^{10}, $H^{5'}$(w)
$H^{3'}$	$H^{4'}$, $H^{3''}$
$H^{4'}$	$H^{3'}$, $H^{5'}$
$H^{5'}$	H^3, H^4, H^5, H^6, $H^{4'}$, $H^{7'}$
$H^{7'}$	H^1, H^3, H^6, H^8, H^9, H^{10}, $H^{5'}$, $H^{9'}$(w)
$H^{9'}$	H^1, H^3, H^6, H^8, H^9, H^{10}, $H^{7'}$(w)
$H^{3''}$	$H^{3'}$, $H^{4''}$
$H^{4''}$	$H^{3''}$, $H^{5''}$
$H^{5''}$	$H^{4''}$, CH_3
CH_3	$H^{5''}$

geometry at each zinc(II) centre. In this complex it is almost impossible to rotate the pyrene rings due to their crossed geometry,[10] and it is certainly more difficult than for **1**, where the offset geometry of the pyrene rings allows the rings to rotate more easily. Thus, there is an entropic cost associated with the formation of the helical complex **1a**, compared to the non-helical complex **1**.

In methanol, compound L^2 forms two complexes with zinc(II) in the ratio **2a**:**2b** = 60:40, while L^3 forms two complexes **3a** and **3b** in approximately equal amounts. The relative amounts of each complex were solvent dependent (Fig. 7). Complexes **2a** and **3a** were assigned as helical, on the basis of model building, which shows that it is more difficult to rotate the aromatic spacers (naphthalene, benzene) than in the corresponding non-helical complexes **2b** and **3b** respectively. Hence selective broadening of the naphthalene protons in **2a** and the benzene

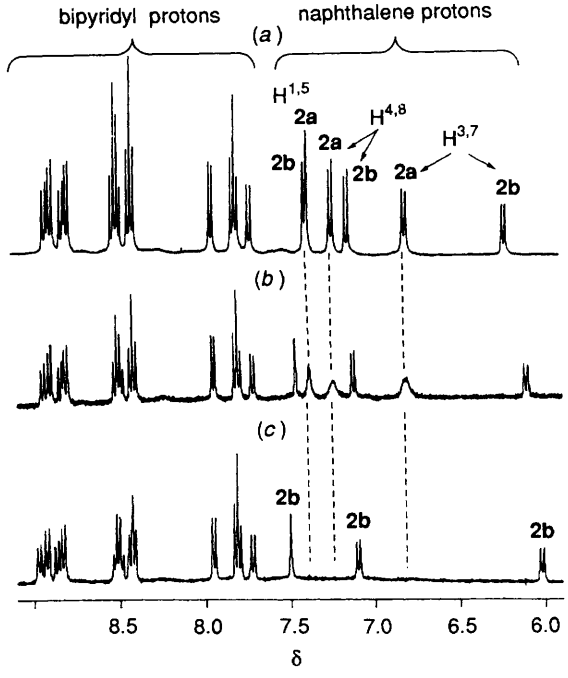

Fig. 5 Proton NMR spectra of complex **2** (400 MHz, CD_3OD) at (*a*) 298, (*b*) 231 and (*c*) 192 K

protons in **3a** was observed on the NMR time-scale (Figs. 5 and 6). Low-temperature NOESY experiments on **2** and **3** did not provide further data to distinguish the helical and non-helical complexes, and previous experiments on **2** with chiral shift reagents did not resolve the chiral helical complex **2a**.

Relative Stabilities of Complexes.—The relative amounts of helical and non-helical complexes formed by compounds L^1–L^3 and zinc(II) are summarized in Fig. 7. With the smallest aromatic linker benzene the stabilities of the two types of complexes are approximately the same. With the slightly larger naphthalene bridge the helical complex **2a** predominates, while for pyrene exclusive formation of the non-helical complex **1** is observed.

Steric effects appear to play a major role in determining the relative amounts. Thus, the large size of the pyrene ring in **1** precludes formation of the helical complex **1a**, in which the rings would be forced into very close proximity to one another and would be unable to rotate. When the size of the spacer is reduced to that of benzene the aromatic rings can rotate in both the helical and non-helical complexes and hence **3a** and **3b** are formed in approximately equal amounts. The skewed nature of the naphthalene spacer in **2** makes it difficult to compare the results obtained with those of complexes **1** and **3**, in which the linkers are symmetric and the complexes have a symmetry axis perpendicular to the aromatic spacers. However, as in the case of **1** and **3**, the formation of different amounts of **2a** and **2b** is most likely a result of the relative contributions of steric effects in these complexes.

The second potential contribution to the stabilities of the complexes that was considered is π–π interactions. These interactions have been shown to be important in the assembly properties of oligopyridyl ligands containing between two and six pyridyl groups with a range of metal ions; however, there are several examples of the efficient assembly of helical complexes in which π-stacking interactions have been shown to be negligible.[4,5] Hunter and Sanders[17] have discussed the nature of π–π interactions and highlighted the importance of offset geometries in aromatic systems. In the crystal structure of complex **1** an offset, stacked geometry of the pyrene rings is

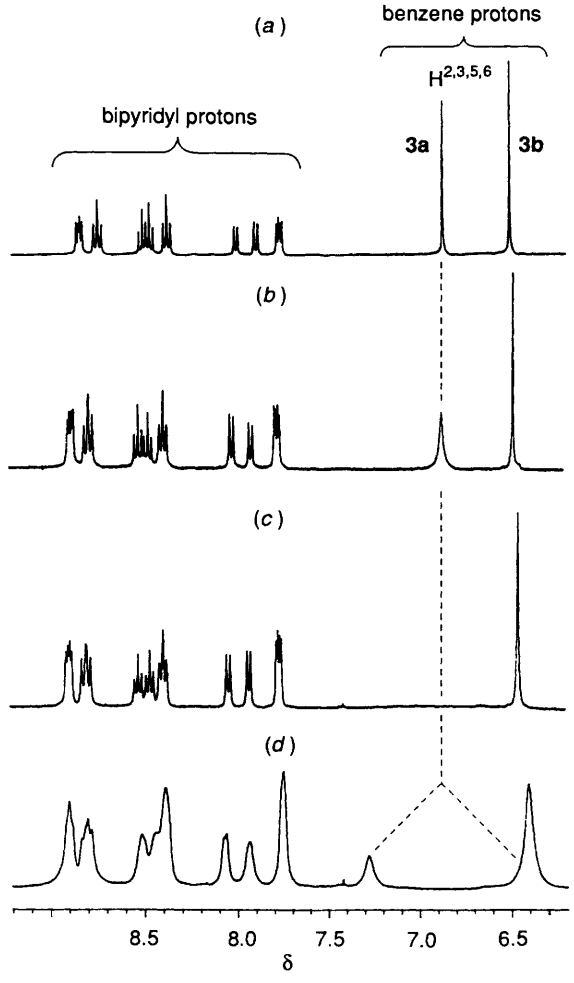

Fig. 6 Proton NMR spectra of complex **3** (400 MHz, CD_3OD) at (*a*) 298, (*b*) 220, (*c*) 187 and (*d*) 170 K (broadness due to solvent viscosity)

observed (Fig. 1). However, maximum overlap of the pyrene rings is not achieved as the zinc(II) co-ordination sphere causes a large lateral offset between the rings. The structure shows some resemblance to that of [4.4](2,7)pyreneophane **I**,[18] but while the interpyrene distances in **1** and **I** are comparable, the lateral offset of the rings in **I** is much less (1.1 Å). Hence, the contribution of π–π interactions to the stability of **1** is minimal and probably not significant. In the helical complex **1a**, which is not formed, the pyrene rings are crossed, and favourable edge-to-edge or face-to-face geometries are not readily achieved. With complexes **2** and **3** there is very little overlap of the aromatic rings and hence π–π interactions were ruled out as a significant contributor to the stability of the complexes. It is noted, however, that edge-to-face geometries are possible in complex **3**.

While the focus of most recent research has been in the area of controlled assembly of double and triple helical structures, the formation of non-helical complexes has been reported in several studies. Sauvage and co-workers[19] observed that 2,9-disubstituted phenanthrolines separated by four carbons, in the presence of Cu^I, form a mixture of helical and non-helical complexes in the ratio 1:8. Williams and co-workers[6–8] have studied the co-ordination chemistry of designed bis(benzimidazole) compounds, and have noted the formation of a double helical complex with Cu^I as well as a non-helical structure which displays weak intramolecular stacking between the benzene linker groups. Constable *et al.*[4,5] have reported both helical and non-helical complexes of oligopyridine ligands. Understanding the factors that control the assembly of both helical and non-helical structures is essential as the field of metallosupramolecular chemistry expands into the development of new supramolecular structures and devices.[1] This paper reinforces the importance of ligand design in controlling the outcome of the assembly properties of ligands containing more than one bipyridyl and metal ions. The use of octahedral zinc bipyridyl complexes to programme information into the assembly of other supramolecular structures remains to be investigated.

The original aim of this work[10] was to design bimetallic macrocyclic complexes with selective recognition features for charged aromatic substrates. In the present system the participation of the ether oxygens in the co-ordination sphere pulls the aromatic rings within van der Waals distance of one another and thus precludes substrate recognition. The synthesis of related ligands which have been designed to favour exclusive formation of either helical or non-helical structures is underway.

Experimental

The NMR spectra were recorded on a Bruker AMX400 spectrometer in the solvent indicated and were referenced to the residual solvent protons. The spectrometer temperature was calibrated by measurement of the shift difference of methanol.[20] Spectra were recorded over spectral widths of 4000 Hz with quadrature detection employed throughout. Two-dimensional spectra were acquired in the phase-sensitive mode using time-proportional phase incrementation.[15] Data sets resulting from 400–512 increments of t_1 were acquired and zero-filled to 1024 points, with each free-induction decay composed of 2048 data points. The NOESY spectra were recorded using mixing times of 150, 250, 300 and 500 ms. Data were subjected to shifted sine-bell weighting functions in f_1 and f_2 and were baseline corrected where required using Bruker software on a Silicon Graphics Indigo workstation.

Synthesis of Complex **1**.—Complex **1** was prepared as previously described.[10] ^1H NMR (CD_3CN): δ 2.08 (s, CH_3), 3.92 and 4.43 (AX system, *J* 12.2, $H^{9'}$), 5.04 (ABq, *J* 16.3, H^7), 6.98 and 7.44 (2br s, H of pyrene), 7.73 (d, *J* 7.9, $H^{5''}$), 7.88 (d, *J* 7.9, $H^{5'}$), 8.33 (dd, *J* 7.9, $H^{4''}$), 8.56 (dd, *J* 7.9, $H^{4'}$), 8.65 (d, *J* 7.9, $H^{3''}$) and 8.89 (d, *J* 7.9 Hz, $H^{3'}$).

1,4-Bis[3-(6′-*methyl*-2,2′-*bipyridin*-6-*yl*)-2-*oxapropyl*]*benzene* L^3.—Sodium hydride (60% dispersion in oil, 48.6 mg, 1.22 mmol) was added to a solution of 6-hydroxymethyl-6′-methyl-2,2′-bipyridine (162 mg, 0.81 mmol) in tetrahydrofuran (thf) (10 cm^3). The mixture was stirred at room temperature for 2 h and 1,4-bis(bromomethyl)benzene (105 mg, 0.40 mmol) was added. The mixture was stirred for 12 h then quenched with water (10 cm^3). The thf was removed under reduced pressure and the remaining aqueous mixture extracted with chloroform (3 × 20 cm^3). The combined extracts were washed with brine (30 cm^3), dried (Na_2SO_4) and the chloroform was removed under reduced pressure. The yellow residue was recrystallized from ethyl acetate to give compound L^3 as off-white needles (110 mg, 55%), m.p. 146.5–147.5 °C (Found: C, 76.0; H, 6.3; N, 10.9. Calc. for $C_{42}H_{34}N_4O_2$: C, 76.5; H, 6.0; N, 11.1%); ^1H NMR ($CDCl_3$): δ 2.63 (s, CH_3), 4.70 (s, CH_2), 4.77 (s, CH_2), 7.16 (br d, $H^{5''}$), 7.43 (s, H^2, H^3, H^5, H^6), 7.51 (br d, $H^{5'}$), 7.68 (dd, *J* 7.8, $H^{4''}$), 7.82 (dd, *J* 7.8 Hz, $H^{4'}$), 8.17 (br d, $H^{3'}$) and 8.29 (br d, $H^{3''}$). λ_{max}($CHCl_3$, log ε/dm^3 mol^{-1} cm^{-1}): 290.8 (6.45) nm. EI mass spectrum: *m*/*z* 503 (*M* + 1, 3), 319 (6), 185 (18), 184 (100), 182 (11), 169 (4), 93 (6) and 66 (4%).

Reaction of L^3 *with* $Zn(CF_3SO_3)_2$.—Compound L^3 (37 mg, 74 μmol) was added to a solution of zinc triflate (26 mg, 72 μmol) in acetonitrile–chloroform (4:1, 3 cm^3) and the solution was stirred for 3 h. The solvent was removed, chloroform (10 cm^3) was added and the mixture heated at reflux for 5 h. It was filtered, the residue washed with hot chloroform (20 cm^3) and dried under high vacuum to give $[Zn_2L^3{}_2][CF_3SO_3]_4 \cdot 2H_2O$ **3**

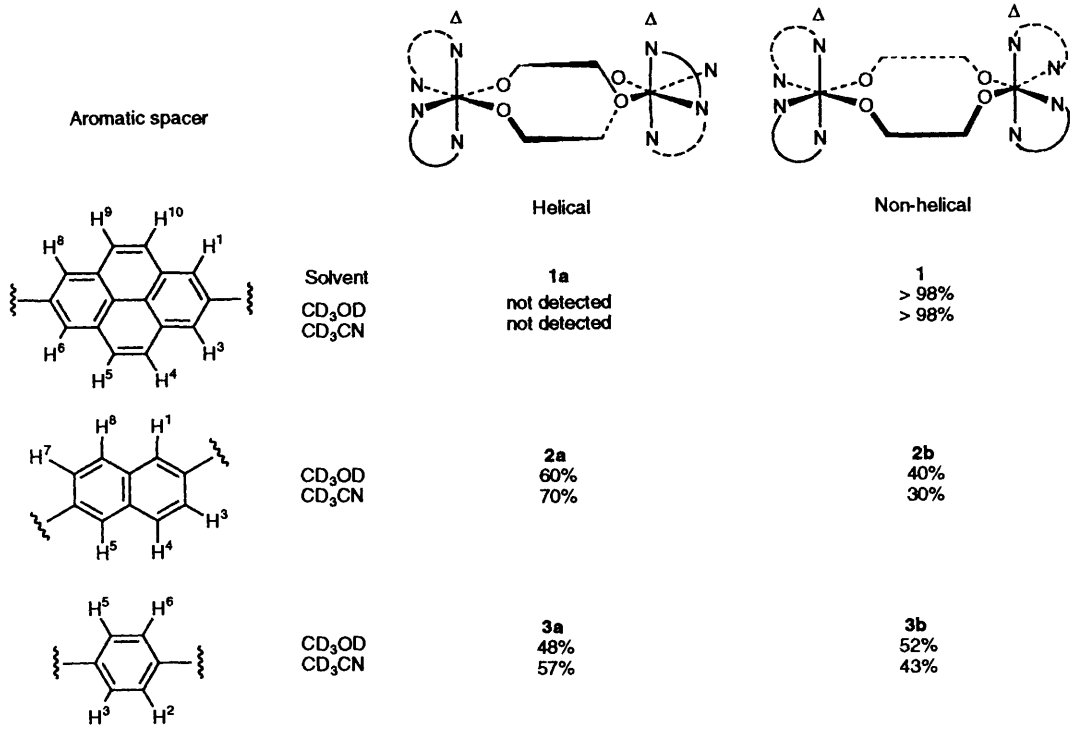

Fig. 7 Relative amounts of helical and non-helical complexes formed between compounds L^1–L^3 and zinc(II)

as a white solid (55 mg, 88%) (Found: C, 45.7; H, 3.9; N, 6.1. Calc. for $C_{68}H_{62}F_{12}N_8O_{17}S_4Zn_2$: C, 46.1; H, 3.6; N, 6.3%); ^{1}H NMR (CD_3CN): **3a**, δ 1.99 (s, CH_3), 3.56 and 3.96 (AX system, *J* 14.0, $H^{9'}$), 4.81 (s, $H^{7'}$), 6.75 (s, H^2, H^3, H^5, H^6), 7.67 (d, *J* 8.0, $H^{5''}$), 7.83 (d, *J* 8.0, $H^{5'}$), 8.29 (dd, *J* 8.0, $H^{4'}$), 8.42 (dd, *J* 7.2, $H^{4''}$), 8.52 (d, *J* 8.0, $H^{3''}$), 8.63 (d, *J* 8.0, $H^{3'}$): **3b**, δ 1.98 (s, CH_3), 3.66 and 4.17 (AX system, *J* 12.4, $H^{9'}$), 4.86 (ABq, *J* 15.9, $H^{7'}$), 6.37 (s, H^2, H^3, H^5, H^6), 7.65 (d, *J* 8.0, $H^{5''}$), 7.74 (d, *J* 8.0, $H^{5'}$), 8.29 (dd, *J* 8.0, $H^{4'}$), 8.37 (dd, *J* 7.2, $H^{4''}$), 8.55 (d, *J* 8.0, $H^{3''}$) and 8.64 (d, *J* 8.0 Hz, $H^{3'}$); λ_{max}($CHCl_3$, log ε/dm^3 mol^{-1} cm^{-1}): 290.4 (4.94), 316 (4.67) and 338.0 (4.87) nm; EI mass spectrum: *m/z* 717 $[M - 2(CF_3SO_3)^-]^{2+}$, 428.3 $[M - 3(CF_3SO_3)^-]^+$, 284 $[M - 4(CF_3SO_3)^-]$ and 252.6 $[1 + 2H]^{2+}$.

X-Ray Crystallography.—Diffraction-quality crystals were grown by slowly infusing diethyl ether into an acetonitrile solution of complex **1**. The crystals decompose within seconds of being removed from the precipitant. Accordingly, a colourless oblong crystal of dimensions 0.43 × 0.08 × 0.03 mm was injected with diethyl ether into a thin-walled glass capillary. Sufficient diethyl ether was removed to expose the crystal and the capillary was then sealed.

Lattice parameters at 21 °C were determined by least-squares fit to the setting parameters of 25 independent reflections, measured and refined on a Rigaku AFC7R four-circle diffractometer employing graphite-monochromated Cu-Kα radiation. Intensity data were collected in the range $4 < \theta < 100°$ using an ω–2θ scan, with a scan width of $(0.74 + 0.35\tan\theta)°$. Data reduction and application of Lorentz, polarization and ψ-scan absorption corrections were carried out using the TEXSAN package.[21] The structure was solved by direct methods using SHELXS 86[22] and the solution was extended by Fourier-difference methods using the TEXSAN program suite. Scattering factors and anomalous dispersion terms used were those incorporated in the TEXSAN package.[21] The limited number of uniquely observed data restricted anisotropic refinement to atoms heavier than the isotropically refined carbon sites. Hydrogen atoms were attached at calculated sites with group isotropic thermal parameters. Two half-occupied oxygen sites and a carbon site, attributable to highly disordered diethyl ether or water molecules located in channels between complexes, were included in the full-matrix refinement. Plots were drawn using ORTEP.[14]

Crystal data. $C_{89}H_{68}F_{12}N_8O_{18}S_4Zn_2$, M = 2024.54, triclinic, space group $P\bar{1}$, a = 16.333(6), b = 18.934(5), c = 10.004(1) Å, α = 100.96(2), β = 97.33(2), γ = 110.71(2)°, U = 2776(1) Å^3, $D_c(Z = 1)$ = 1.211 g cm^{-3}, μ(Cu-Kα) = 19.22 cm^{-1}, λ(Cu-Kα) = 1.5418 Å, $F(000)$ = 1034 electrons. *hkl* Ranges of 0–18, −21 to 21, −11 to 11. N = 4735, N_o = 1916 $[I > 2\sigma(I)]$, N_{var} = 374, R = 0.097, R' = 0.092, w = $1/\sigma(F)^2$ residual extrema 0.2 to 0.4 e Å^{-3}.

Additional material available from the Cambridge Crystallographic Data Centre comprises H-atom coordinates, thermal parameters and remaining bond lengths and angles.

Acknowledgements

Financial support from the Australian Research Council and the Cooperative Research Centre for Molecular Engineering and Technology is gratefully acknowledged.

References

1 E. C. Constable, *Chem. Ind.* (*London*), 1994, 56 and refs. therein; *Nature* (*London*), 1990, **346**, 314; 1993, **362**, 412 and refs. therein.
2 *Perspectives in Coordination Chemistry*, eds. A. F. Williams, C. Floriani and A. E. Merbach, VCH, Weinheim, 1992.
3 J.-M. Lehn, A. Rigault, J. Siegel, J. Harrowfield, B. Chevrier and D. Moras, *Proc. Natl. Acad. Sci. USA*, 1987, **84**, 2565; J.-M. Lehn and A. Rigault, *Angew. Chem., Int. Ed. Engl.*, 1988, **27**, 1095; U. Koert, M. M. Harding and J.-M. Lehn, *Nature* (*London*), 1990, **346**, 339; T. M. Garrett, U. Koert, J.-M. Lehn, A. Rigault, D. Meyer and J. Fisher, *J. Chem. Soc., Chem. Commun.*, 1990, 557; R. Krämer, J.-M. Lehn, A. De Cian and J. Fisher, *Angew. Chem., Int. Ed. Engl.*, 1993, **32**, 703.
4 E. C. Constable and M. D. Ward, *J. Am. Chem. Soc.*, 1990, **112**, 1256; E. C. Constable, *Angew. Chem., Int. Ed. Engl.*, 1991, **30**, 1450.
5 E. C. Constable, S. M. Elder, J. Healy and M. D. Ward, *J. Am. Chem. Soc.*, 1990, **112**, 4590; E. C. Constable, M. J. Hannon and D. A. Tocher, *J. Chem. Soc., Dalton Trans.*, 1993, 1883.

6 A. F. Williams, C. Piguet and G. Bernardinelli, *Angew. Chem., Int. Ed. Engl.*, 1991, **11**, 1490; C. Piguet, G. Bernardinelli and A. F. Williams, *Inorg. Chem.*, 1989, **28**, 2920.
7 C. Piguet, G. Bernadinelli, B. Bocquet, A. Quattropane and A. F. Williams, *J. Am. Chem. Soc.*, 1992, **114**, 7440.
8 S. Rüttiman, C. Piguet, G. Bernardinelli, B. Bocquet and A. F. Williams, *J. Am. Chem. Soc.*, 1992, **114**, 4230.
9 G. Struckmeier, U. Thewalt and J.-H. Fuhrhop, *J. Am. Chem. Soc.*, 1976, **98**, 278.
10 A. Bilyk and M. M. Harding, *J. Chem. Soc., Dalton Trans.*, 1994, 77.
11 C. K. Johnson, ORTEP, A Thermal Ellipsoid Plotting Program, Oak Ridge National Laboratories, Oak Ridge, TN, 1965.
12 See J. M. Harrowfield and S. B. Wild, in *Comprehensive Coordination Chemistry*, ed. G. Wilkinson, 1986, vol. 1, p. 179; D. A. Reitsma and F. R. Keene, *J. Chem. Soc., Dalton Trans.*, 1993, 2859.
13 See, for example, P. J. Burke, D. R. McMillin and W. R. Robinson, *Inorg. Chem.*, 1980, **19**, 1211; K. V. Goodwin, D. R. McMillin and W. R. Robinson, *Inorg. Chem.*, 1986, **25**, 2033.
14 W. Fitzgerald, B. Murphy, S. Tyagi, B. Walsh and B. Hathaway, *J. Chem. Soc., Dalton Trans.*, 1981, 2271.
15 D. Marion and K. Wütrich, *Biochem. Biophys. Res. Commun.*, 1983, **113**, 967.
16 J. Jeener, B. H. Meier, P. Bachmann and R. R. Ernst, *J. Chem. Phys.*, 1979, **71**, 4546; A. Kumar, R. R. Ernst and K. Wütrich, *Biochem. Biophys. Res. Commun.*, 1980, **95**, 1.
17 C. A. Hunter and J. K. M. Sanders, *J. Am. Chem. Soc.*, 1990, **112**, 5525.
18 H. A. Stabb, N. Riegler, F. Diederich, C. Krieger and D. Schweitzer, *Chem. Ber.*, 1984, **117**, 246.
19 C. O. Dietruch-Buchecker, J.-P. Sauvage, J.-P. Kintzinger, P. Maltese, C. Pascard and J. Guilhem, *New J. Chem.*, 1992, **16**, 931.
20 A. L. Van Geet, *Anal. Chem.*, 1970, **42**, 679.
21 TEXSAN, Single Crystal Structure Analysis Software, Version 1.6, Molecular Structure Corporation, The Woodlands, Houston, TX, 1993.
22 SHELXS 86, G. M. Sheldrick, in *Crystallographic Computing 3*, eds. G. M. Sheldrick, C. Krüger and R. Goddard, Oxford University Press, 1985, pp. 175–188.

Received 12*th April* 1994; *Paper* 4/02169J